Gene Therapy (2007) 14, 733–740

www.nature.com/gt

ORIGINAL ARTICLE

AAV-mediated delivery of a mutated myostatin propeptide ameliorates calpain 3 but not α-sarcoglycan deficiency

M Bartoli[1], J Poupiot[1], A Vulin, F Fougerousse, L Arandel, N Daniele, C Roudaut, F Noulet, L Garcia, O Danos and I Richard
Généthon, CNRS UMR8115, Evry, France

Myostatin is a negative regulator of muscle mass whose inhibition has been proposed as a therapeutic strategy for muscle-wasting conditions. Indeed, blocking myostatin action through different strategies has proved beneficial for the pathophysiology of the dystrophin-deficient mdx *mouse. In this report, we tested the inhibition of myostatin by AAV-mediated expression of a mutated propeptide in animal models of two limb-girdle muscular dystrophies: LGMD2A caused by mutations in the calpain 3 (CAPN3) gene and LGMD2D caused by mutations in the α-sarcoglycan gene (SGCA). In the highly regenerative* Sgca*-null mice, survival of the α-sarcoglycan-deficient muscle fibers did not improve after transfer of the myostatin propeptide. In calpain 3-deficient mice, a boost in muscle mass and an increase in absolute force were obtained, suggesting that myostatin inhibition could constitute a therapeutic strategy in this predominantly atrophic disorder.*
Gene Therapy (2007) **14,** 733–740. doi:10.1038/sj.gt.3302928; published online 1 March 2007

Keywords: *limb-girdle muscular dystrophies; α-sarcoglycan; calpain 3; myostatin propeptide; AAV; gene transfer*

Introduction

Myostatin (growth differentiation factor-8) is a secreted growth factor belonging to the transforming growth factor-β (TGF-β) superfamily that acts as a negative regulator of skeletal muscle mass. A number of natural, inactivating mutations have been identified in cattle, mouse, sheep and human, all leading to a hypermuscular phenotype.[1–6] The biological relevance of myostatin was also addressed in mice by gene inactivation, overexpression of normal or dominant-negative forms and systemic administration of inactivating antibody or myostatin protein.[7–15] From these studies and many others carried out in cultured cells, the general opinion is that myostatin regulates the final number of muscle fibers during development by blocking the proliferation and differentiation of myoblasts and also regulates the postnatal muscle-fiber size by maintaining the satellite cells in a quiescent state and inhibiting protein synthesis.[16,17]

Myostatin is synthesized as a 375-amino acids precursor composed of a signal sequence at the N-terminus, a 28 kDa propeptide region and a 12 kDa 'mature' region at the C-terminus.[16,17] After proteolytic processing of this precursor, myostatin is secreted as an inactive latent complex of a disulfide-bond carboxy terminal dimer bound to the propeptide or other myostatin-binding proteins.[18] It has been suggested that one mechanism for activating myostatin consists of the proteolytic cleavage of the propeptide at the residue D76 by members of the bone morphogenetic protein-1/tolloid (BMP-1/TLD) family of metalloproteinases.[19] Following activation, the mature region binds to activin transmembrane receptors, which in turn initiate an intracellular signaling cascade, involving Smad proteins and leading to targeted gene transcription.[20,21]

Considering its effect on muscle growth, inhibition of myostatin has been proposed as a therapeutic approach in muscle-degenerative and wasting conditions, such as muscular dystrophies and cachexia.[22–25] Indeed, improvement of the pathological signs of the dystrophin-deficient *mdx* mice model was obtained after crossing with myostatin null mice or after systemic injection of neutralizing monoclonal antibodies or a stabilized propeptide.[26–28] However, doubts have been raised whether myostatin inhibition leads to a truly healthy muscle as exercise in myostatin-deficient cattle led to early exhaustion.[29] Furthermore, it can even be deleterious as disused muscle atrophy is markedly more severe in the context of myostatin deficiency[30] and as crossing laminin-deficient dy(W) mice model with myostatin null mice led to an increased mortality.[31] These observations suggest that each individual situation has to be tested to define if they could benefit from myostatin blockade.

In this report, we investigated the effect of myostatin inhibition using a propeptide mutated at residue D76 on the pathophysiology of two animal models of recessive limb-girdle muscular dystrophies, LGMD2A (OMIM

Correspondence: Dr I Richard, Généthon, CNRS UMR8115, 1 rue de l'internationale, 91000 Evry, France.
E-mail: richard@genethon.fr
[1]These authors contributed equally to this work.
Received 3 August 2006; revised 3 October 2006; accepted 20 December 2006; published online 1 March 2007

253600) and LGMD2D (OMIM 608099). LGMD2A is due to mutations in the muscle-specific cysteine protease calpain 3, the function of which is not fully deciphered but seems important for the correct homeostasis of the sarcomere.[32] LGMD2D is due to mutations in α-sarcoglycan, a transmembrane-protein part of the complex associated with dystrophin.[33–35] Adeno-associated virus (AAV)-mediated expression of the mutated form of the myostatin propeptide in the muscles of these two models led to different outcomes. In the highly regenerative *Sgca*-null mice, survival of the α-sarcoglycan-deficient muscle fibers did not improve after transfer of the myostatin propeptide. In calpain 3-deficient mice, a boost in muscle mass and an increase in absolute force were obtained, suggesting that myostatin inhibition could constitute a therapeutic strategy in this predominantly atrophic disorder.

Results

Effect of a mutated propeptide on muscle growth of normal mice

To obtain a myostatin propeptide that would have a more potent inhibitory effect on myostatin, we mutated the propeptide at the BMP-1/TLD cleavage site by replacing the aspartate at position 76 by an alanine residue (D76A). In addition, we replaced the signal sequence of the propeptide by the coding sequence of the murine-secreted alkaline phosphatase (mSeAP) to monitor the expression and secretion of the transgene. This construct was inserted into a rAAV2/1 vector under control of the cytomegalovirus (CMV) promoter to obtain the rAAV2/1-mSeAP-propmyoD76A vector (Figure 1). A vector devoid of the propeptide (AAV2/1-mSeAP) was used as a control (Figure 1).

Two-month-old 129SV male mice were injected in the left tibialis anterior (TA) muscles either by rAAV2/1-mSeAP-propmyoD76A or the control rAAV2/1-mSeAP vectors. To verify that the presence of the propeptide at the C-terminus of mSeAP did not impair the phosphatase activity or prevent the secretion of the fused protein, we quantified mSeAP in blood from the injected animals and carried out phosphatase staining on muscle slices at the end point of the experiment. Six weeks after injection, a high number of positive fibers were observed throughout the muscle with both vectors (Figure 2a). This efficient transduction was associated with significant amounts of mSeAP in blood samples, indicating that the fusion is permissive for the secretion of mSeAP (Figure 2a). However, we noticed a higher intensity in fiber staining but a weaker blood level of mSeAP with rAAV2/1-mSeAP-propmyoD76A compared with rAAV2/1-mSeAP, suggesting that the secretion is not as efficient as in the former case.

To assess the effect of the expression of this construct on muscle growth, muscles were weighted at the end point of the experiment. Those injected with the rAAV2/1-mSeAP-propmyoD76A showed a mean increase of

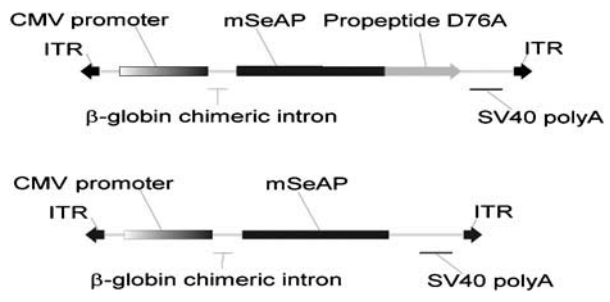

Figure 1 Diagram representing the AAV virus genomes used in this study.

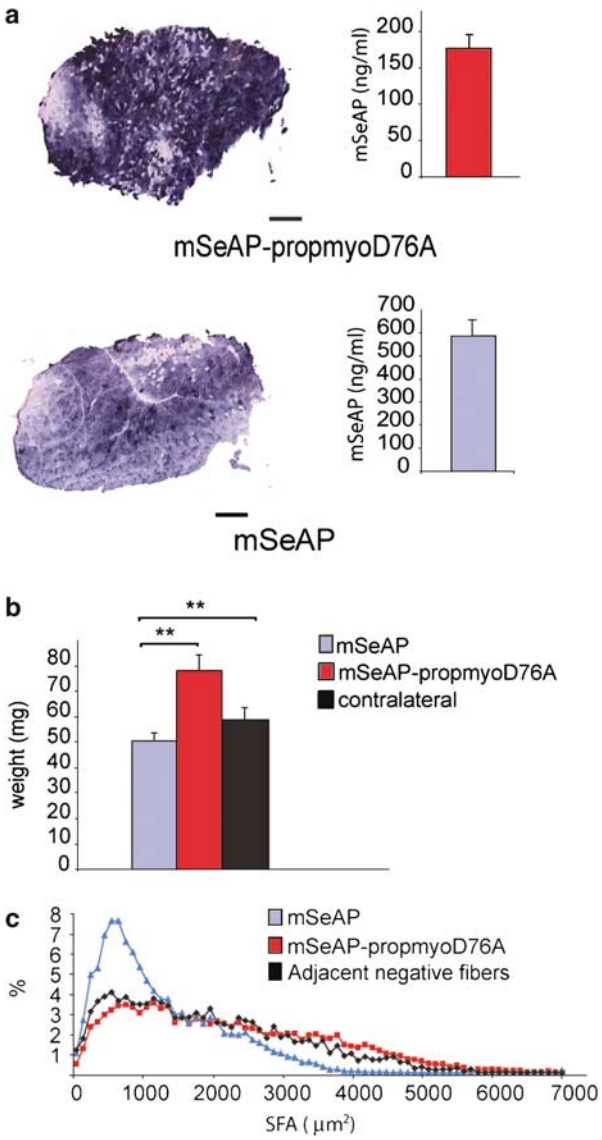

Figure 2 (**a**) Detection of mSeAP 6 weeks after intramuscular injection of rAAV2/1-mSeAP-propmyoD76A and rAAV2/1-mSeAP into the TA of WT mice. Left panels: *in situ* mSeAP detection on muscle sections using the NBT/BCIP method and counterstained with H&E. Positive fibers for mSeAP are dark blue. Scale bars represent 150 μm. Right panels: Histogram presenting the serum levels of the mSeAP protein (ng ml^{-1}) in WT mice injected with rAAV2/1-mSeAP-propmyoD76A or rAAV2/1-mSeAP. Values are mean plus s.d. with $n=4$. (**b**) histogram showed the mean weight of the muscles injected with rAAV2/1-mSeAP or rAAV2/1-mSeAP-propmyoD76A and its contralateral. (**c**) Histograms representing the frequency of the SFA showed that mSeAP-propmyoD76A expression induced an increase in the mean fiber size of the muscles ($n=4$). The black curve represents the mean fiber SFA for mSeAP negative fibers in injected muscles.

muscle mass of 60% compared with rAAV2/1-mSeAP-injected muscles (75.88±5.99 versus 47.23±1.32; $P=0.01$; Figure 2b). These results indicated that the fused propeptide was efficient in inducing growth in the injected muscle. In addition, it should be noted that the contralateral muscle of mice injected with rAAV2/1-mSeAP-propmyoD76A showed a significant increase of 15% compared with rAAV2/1-mSeAP-injected muscles (54.75±4.37; $P=0.01$; Figure 2b), indicating that the mutated propeptide had a weaker but real endocrine effect.

To determine whether this increase was due to hypertrophy or hyperplasia, we measured the number of fibers and the single fiber area (SFA). No significant change in the number of fibers between both groups was observed (rAAV2/1-mSeAP-injected TA: 3363±454 and rAAV2/1-mSeAP-propmyoD76A-injected TA: 3055±182; $P=0.336$). However, we observed a 78% augmentation ($P=0.002$) of the SFA from 1236±108 μm^2 for rAAV2/1-mSeAP to 2196±192 μm^2 for rAAV2/1-mSeAP-propmyoD76A (Figure 2c). Detailed morphometric analyses of mSeAP negative fibers adjacent to positive fibers showed that these fibers had also undergone an increase in size, indicating that there is a paracrine effect of the propeptide (Figure 2c). As observed for the weight, a small increase was detected for the contralateral muscle (1586±167 μm^2; $P=0.038$ versus mSeAP-injected muscles).

Injection of the mutated propeptide in two animal models of limb-girdle muscular dystrophies

Having demonstrated the ability of mSeAP-propmyoD76A to induce muscle growth, we assessed its beneficial effect on pathology in α-sarcoglycan and calpain 3-deficient mice. Considering the benefit brought by myostatin inhibition in the *mdx* mice and the participation of α-sarcoglycan in the dystrophin-associated complex, we postulated that myostatin inhibition could be equally beneficial in the *Sgca*-null model. In addition, we speculated that myostatin inhibition could reverse the atrophic phenotype of the calpain 3-deficient mice.

We injected rAAV2/1-mSeAP-propmyoD76A or rAAV2/1-mSeAP into the left TA muscle of male mice of these models. To verify that the mSeAP-propmyoD76A was also correctly expressed and secreted after intramuscular injection, we measured the amount of mSeAP in blood and sampled the muscles of the anterior compartment of the limbs at the end of the experiment (6 weeks after the injection). Unexpectedly, the level of mSeAP activity in the blood of *Sgca*-null mice hardly rose above the background level after injection of rAAV2/1-mSeAP-propmyoD76A (10 ng/ml; Figure 3a). This low level of mSeAP was correlated with an expression in very few fibers as seen in a cross section of a representative left muscle (Figure 3b). In contrast, an mSeAP secretion of intensity comparable to that observed in the data obtained with wild-type (WT) mice was observed in calpain 3-deficient mice (Figure 3a; 263 ng ml^{-1} for the calpain 3-deficient mice compared with 176 ng ml^{-1} for control mice; $P=0.1$). This secretion was associated with a large number of fibers expressing the transgene on muscle cross sections (Figure 3b).

As expected from the absence of mSeAP expression, the injected muscles of *Sgca*-null mice did not increase

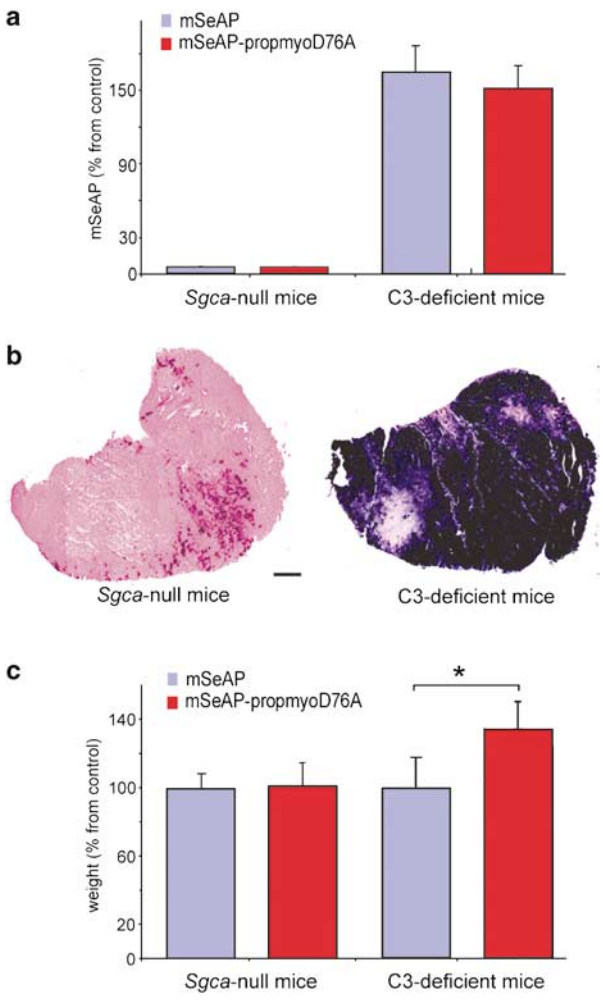

Figure 3 Analysis of α-sarcoglycan and calpain 3-deficient muscles after AAV-mediated injection of the propeptide. (**a**) Histogram representing the percentage of mSeAP in blood from *Sgca*-null and calpain 3-deficient mice injected either by rAAV2/1-mSeAP-propmyoD76A or rAAV2/1-mSeAP compared with control mice (100%). (**b**) Staining for mSeAP on frozen muscle sections injected with rAAV2/1-mSeAP-propmyoD76A brought to light the small number of positive fibers in *Sgca*-null muscle, but a wide and high level of expression in calpain 3-deficient muscles. Black scale bar represents 150 μm. (**c**) Mean weights of muscle increase compared with mSeAP-injected muscles. rAAV2/1-mSeAP-PropmyoD76A injection did not induce an increase of muscle mass in *Sgca*-null muscles, but a 31% increase of muscle mass in calpain 3-deficient muscles (*$P<0.05$).

in mass (Figure 3c), nor were they improved in their susceptibility to necrosis as monitored by Blue Evans staining (data not shown). Considering the absence of hypertrophic benefit in the highly regenerative *Sgca*-null mice, we did not further analyze these mice. In contrast, the high level of expression obtained with the calpain 3-deficient mice was associated with an increase of 31% in the mass of the injected muscles compared with the mSeAP-injected muscles (59.03±4.8 versus 44.87±4.43; $P=0.04$; Figure 3c).

Effect on the pathology in the calpain 3-deficient mice

The morphological analyses carried out on calpain 3-deficient mice limbs showed that the total number of fibers was not significantly different after treatment

(3210±401 versus 3557±312; $P=0.529$). However, the SFA increased about 54% (1838±157 versus 1195±151 μm^2 for mSeAP; $P=0.007$), indicating that the hypertrophic phenotype was mainly because of an increase in fibers size as observed in WT animals (Figure 4a). No drastic improvement of the histology of the treated muscles was noticed (Figure 4b). As calpain 3 deficiency has been proposed to alter the maturation of the muscle fibers by delaying sarcomere formation,[36] we labeled control and treated muscles with a developmental form of myosin heavy chain (MHCd). No difference was detected between injected and non-injected muscles (Figure 4c). Specifically, we did not detect any accumulation of MHCd-positive fibers over time in calpain 3-deficient muscles.

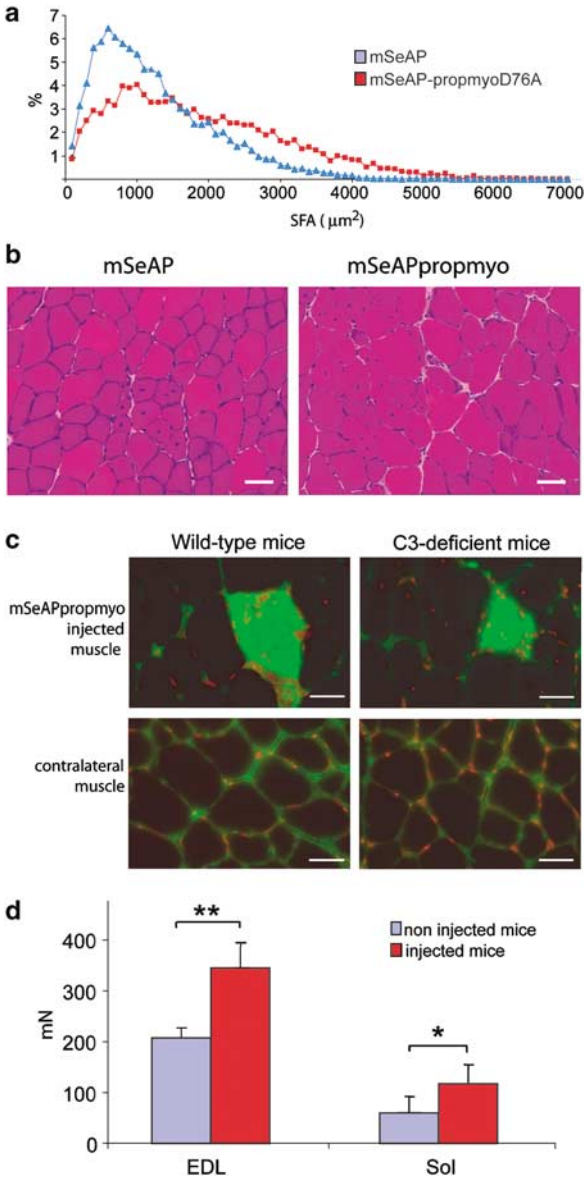

Figure 4 Analysis of calpain 3-deficient muscles after intramuscular (**a**–**c**) and intra-arterial (**d**) AAV-mSeAP-propmyoD76A injections. (**a**) Histograms showed that mSeAP-propmyoD76A expression induced an increase in the mean SFA ($n=4$). (**b**) No obvious difference was observed between rAAV2/1-mSeAP and rAAV2/1-mSeAP-propmyoD76A-injected calpain 3-deficient mice on H&E staining. (**c**) MHCd staining of muscle sections from mice injected with rAAV2/1-mSeAP-propmyoD76A or rAAV2/1-mSeAP. It should be noted that, in both cases, the MHCd-positive fibers are large fibers indicative of fusion of newly activated satellite cells to pre-existing fibers rather than formation of new fibers. This observation is consistent with the absence of increase in the total number of fibers. Scale bars represent 50 μm. (**d**) Histograms representing the mean contractile absolute tetanic force of the EDL from non-injected and rAAV2/1-mSeAP-propmyoD76A-injected calpain 3-deficient mice ($n=6$) (*$P<0.01$; **$P<0.001$).

To test if mSeAP-propmyoD76A-induced hypertrophy could strengthen calpain 3-deficient muscles, we performed a femoral intra-arterial injection of the rAAV2/1-mSeAP-propmyoD76A in 5-month-old males. An increase in the mass of muscles was observed after injection of rAAV2/1-mSeAP-propmyoD76A (TA 47.3%, $P=0.002$; gastrocnenius 38%, $P=0.011$; quadriceps 24%, $P=0.01$ and extensorum digitorum longus (EDL) 48.3%; $P=0.001$). However, this increase did not reflect on the body weight ($P=0.26$).

EDL and soleus muscles were then processed for *in vitro* analysis of contractile force as described previously.[37] The maximum absolute isometric tetanic force was 341±56 mN in EDL from rAAV2/1-mSeAP-propmyoD76A-injected limbs versus 208±32 mN ($P<0.001$) from mSeAP-injected limbs (Table 1 and Figure 4c). The maximum absolute isometric tetanic force was 114±45 mN in soleus from rAAV2/1-mSeAP-propmyoD76A-injected limbs versus 61±12 mN ($P=0.005$) from mSeAP-injected limbs (Table 1 and Figure 4d). However, when the force was normalized for the muscle cross-sectional area (specific isometric tetanic force), the difference fell below the limit of significance (Table 1). It can also be noted from these analyses that T_{50} (half relaxation time of tetanus), an indicator reflecting the composition of fiber, was not modified (Table 1).

Discussion

We treated *Sgca*-null and calpain 3-deficient mice with a recombinant AAV encoding a mutated propeptide to determine whether myostatin inhibition could alleviate the pathological signs in these models. We observed different outcomes depending on the deficiencies with a boost of the muscle mass associated with an increase of the force of the muscle obtained only in calpain 3-deficient mice.

The propeptide used in this study was mutated at the proteolytic cleavage site between R75 and D76. A cleavage in this region was shown to induce propeptide release from myostatin, hence resulting in activation of the latent complex.[19] Indeed, cleavage of the propeptide by BMP-1/TLD at this location was proposed to be an activation mechanism of myostatin,[19] but this has yet to be demonstrated *in vivo*. It is interesting to note that one study reported that injection of Fc-fused propeptide is effective in inducing hypertrophy in WT female mice only when mutated at the corresponding residue.[19] In our experiments, rAAV-mediated injection of the mutated propeptide induced hypertrophy to an extent overrating both what we obtained with a WT propeptide (a 20–30% increase; data not shown) and what was reported in the literature in normal adult mice.[12] These elements suggest that the presence of the mutation could indeed be considered an advantage. However, additional

Table 1 Isolated muscle kinetic properties of EDL and soleus in calpain 3-deficient mice injected with rAAV2/1-propmyoD76A ($n=6$) compared with untreated ($n=12$)

	Isometric contraction					
	EDL			*Soleus*		
	Force (mN)	*Tension (mN/mm²)*	T_{50}	*Force (mN)*	*Tension (mN/mm²)*	T_{50}
rAAV-propmyoD76A	341±56	146±21	40±3.5	114±45	120±45	108±13
Untreated	208±32	125±24	40.6±4	61±12	88±23	100±10
P-value	1.3 e-5	0.1	0.7	0.005	0.09	0.2

Abbreviation: EDL, extensorum digitorum longus.
Parameters are presented as means±s.d. Tension is the normalized tetanic force. T_{50} is the half relaxation time of tetanus.

experiments would be needed to fully comprehend whether the mutation would make any difference depending on the mode of propeptide delivery, the duration of its presence in the organism and/or the physiological or pathological condition of the muscle.

Using injection of rAAV2/1-propmyoD76A for blockade of myostatin is inefficient in the *Sgca*-null mice. The level of expression obtained with this vector is equivalent to the expression of a reporter transgene, such as mSeAP and much lower than a therapeutic one injected at the same age.[38] As an explanation, it can be suggested that any propeptide that may be expressed in fibers did not circumvent the membrane-related degenerative process. This hypothesis is consistent with the absence of reversal of stretch sensitivity observed in the *mdx* mice after pharmacological blockade of myostatin,[26,28] suggesting that membrane destabilization persists even if the muscle is stronger. Alternatively, considering that we used a ubiquitous promoter to drive the expression of mSeAP, it is possible that an immune response was elicited in the highly inflammatory muscle tissue of the *Sgca*-null mice. Whatever the hypotheses, a clearance of the vector from the tissue is ultimately achieved. Nonetheless, whereas the present strategy was proved to be inefficient, it remains to be seen if other approaches using expression from another organ or with a different mode of action, such as the use of neutralizing antibody could be beneficial for α-sarcoglycan deficiency, as it has been shown in *mdx* mice.[26,28]

In contrast to the situation with the *Sgca*-null mice, inhibition of myostatin in the calpain 3-deficient model not only induced muscle growth but also increased the absolute tetanic force of the muscle. The positive effect obtained in this case compared with what was observed in the *Sgca*-null mice can be put in relation to the difference in turnover of fibers in those two deficiencies, reflecting a distinction in the pathophysiological mechanisms. For *Sgca*-null mice, the loss of α-sarcoglycan at the membrane leads to leakiness of the membrane, excess of calcium influx, aberrant activation of calcium-dependent proteases, unwanted proteolysis and finally cell death. For the calpain 3-deficient model, the pathophysiological mechanism is less clear, considering that the function of this protease is not fully understood. However, it seems that calpain 3 is necessary for remodeling of the cytoskeleton, leading, in case of deficiency, to abnormal sarcomeres associated with an increase in cellular stress.[31] In contrast with the human situation where these events seem to induce an increase in cell death by apoptosis, it is less clear that it occurs in mice, explaining the low rate of turnover.

The level of forces obtained after transfer even exceeds that achieved after AAV-mediated *calpain 3* gene transfer.[39] *Calpain 3* was proposed to participate in the maturation and growth of the muscle fibers, as its deficiency induced a delayed sarcomere formation and a decrease of the rate of mass recovery following hindlimb suspension.[36,40] Considering this hypothesis and as increase in muscle mass and augmentation of force of the individual myofibers necessitates new incorporation of sarcomeres, it was not *a priori* evident that myostatin inhibition would be efficient in the absence of *calpain 3*. In fact, we observed that the level of growth of individual myofibers was not significantly different between WT- and *calpain 3*-deficient muscles (analysis of variance (ANOVA): $P=0.09$) even if growth seems less efficient than in WT animals when the whole muscle is considered (ANOVA analysis: $P=0.02$). This discrepancy could be related to the dystrophic state of the muscle tissue, which includes a non-responsive fraction constituted by fibrosis and inflammatory infiltrates. In addition, results of the tension and T_{50} indicated that muscle growth in the context of calpain 3 deficiency is not associated with a drastic modification of mechanistic quality of the sarcomere. This, together with the absence of accumulation of MHCd-positive fibers, seems to indicate that the increase of muscle mass induced by myostatin inhibition is not associated with deleterious myofibrillogenesis in the context of calpain 3 deficiency. Altogether, the positive effects on the atrophy and force shown herein are encouraging for the use of myostatin inhibition to alleviate the LGMD2A symptoms, widening the possible application of this strategy.

Materials and methods

Vector construction and production

To construct the pAAV-CMV-mSeAPpropmyoD76A, the coding sequence of mSeAP (without the stop codon) was amplified from the pVT20 plasmid (a gift from Vincent Thuiller[41]) with oligonucleotides VT20-F-*Xho*I 5′-CCGCT CGAGCGGATGTGGGGAGCCTGCTTGCT-3′ and SeAP-R-*Kpn*I 5′-GGGGTACCGCCCGGGCTCACTGCACTGCT-3′ and subcloned using Zero Blunt TOPO PCR Cloning Kit (Invitrogen, Paisley, UK), generating the plasmid pCR-SeAP.

The propeptide sequence of myostatin with its sequence signal deleted was also subcloned by TOPO cloning to generate the pCR-PropMyo plasmid after amplification with oligonucleotides MusPro-*Kpn*I-F 5′-GGGGTACCTGTAATGCATGTGCGTGGAGA-3′ and MusPro-BamHI-R 5′-CGCGGATCCCCTATTAGTCTCTC CGGGACCTCTT-3′ on a pAAV plasmid, where the propeptide was previously cloned from murine skeletal muscle cDNA. The mutation D76A was introduced in this plasmid using QuikChange Site-Directed Mutagenesis kit (Stratagene, La Jolla, CA, USA) with the primers D76A.up: 5′-CAGTACGACGTCCAGAGGGCT GACAGCAGTGATGGCTCT-3′ and D76A.bot: 5′-AGAG CCATCACTGCTGTCAGCCCTCTGGACGTCGTACTG-3′.

The plasmid pAAV-CMV-mSeAPropmyo was then constructed by successively subcloning a *Xho*I–*Kpn*I fragment containing the mSeAP coding sequence from pCR-SeAP and a *Kpn*I–*Kpn*I fragment containing the myostatin propeptide from pCR-Propmyo into an AAV-based pSMD2-derived vector.[42] The plasmids pAAV-mSeAP and pAAV-CAPN3 were previously described.[39,43]

Plasmid DNA was prepared using the EndoFree Megaprep kit (Hoerdt, France) from Macherey-Nagel. All constructs were subjected to automated sequencing to verify integrity of the constructs. Adenovirus-free AAV2/1 viral preparations were generated by packaging AAV2-ITR recombinant genomes in AAV1 capsids using a three plasmid transfection protocol.[44] Physical particles were quantified by a quantitative TaqMan assay.[45]

Animal experiments

A murine knockout for α-sarcoglycan was obtained from K Campbell (Howard Hughes Medical Institute, Iowa City, IA, USA). The construction and characterization of this model was previously described.[46] The construction and characterization of calpain 3-deficient model was previously described.[37,47] Control male mice from the 129SV strains were purchased from Charles River Laboratories (Les Oncins, France). All mice were handled according to the European guidelines for the humane care and use of experimental animals.

For intramuscular injection, 129SV or deficient mice were injected with 25 μl (6 to 1.3×10^{10} viral genomes (vg) per injection) of rAAV viral preparation at the age of 2 months for WT and calpain 3-deficient mice and at the age of 5 weeks to 2 months for *Sgca*-null mice. Detailed procedure for intra-arterial injection was previously described.[48] Briefly, anesthetized mice underwent femoral artery and vein isolation of the right hindlimb. After clamping the femoral vein and two collaterals, a catheter was introduced in the femoral artery and the rAAV preparation (2.5×10^{12} vg per injection) was injected in a volume of 1 ml 20^{-1} g of body weight at a rate of 100 μl s^{-1}.

Blood samples were obtained every week by retro-orbital puncture of anesthetized animals. Detection of mSeAP in those samples was carried out as described previously.[39]

The EDL and SOL muscles were surgically excised for measurement of isometric contractile properties *in vitro*, maintained in Krebs buffer and processed as described previously.[37] The following parameters were studied: P_0, the maximum tetanic force and T_{50}, the duration to a P_0 decrease by 50%. Isometric tension was calculated by dividing the force by estimated cross-sectional area of the muscle.

Immunofluorescence, histological and morphometric analyses

Cryosections (8 μm thickness) were prepared from frozen muscles. Transverse sections were processed for hematoxylin and eosin (H&E) histological staining. Detection of mSeAP on muscle slices were carried out as described previously.[39]

For immunohistochemical detection of MHCd-positive fibers, cryosections were blocked with phosphate buffered saline (PBS)+10% goat serum for 1 h and then incubated in a humid chamber with a 1/40 dilution of primary antibody (NCL-MHCd, Novocastra, Antony, France) for 1 h at room temperature (RT). After washing with PBS 1 ×, sections were incubated with a goat anti-mouse secondary antibody conjugated with Alexa488 (Molecular Probes, Paisley, UK) dye-diluted 1/1000 (A-11070, Molecular Probes) for 1 h at RT. Sections were mounted with Fluoromount-G (Cliniscience, Montrouge, France) after 4,6-diamidino-2-phenylindole (DAPI) staining and visualized on a Leica confocal fluorescence microscope. For immunohistochemical staining of slow-type fibers, an antibody against the skeletal slow myosin (M8421, Sigma, Lyon, France) was used and the detection was carried out according to the ARK peroxidase kit (Dako, Trappes, France).

For morphological analysis, unfixed transverse cryosections were treated for 20 min with H_2O_2 to inhibit endogenous peroxidase, blocked with PBS+10% goat serum for 30 min and then incubated with 1/400 dilution of polyclonal rabbit anti-laminin primary antibody (10765, Progen) for 2 h at RT. After washing with PBS, sections were incubated with a goat anti-rabbit HRP-labeled antibody (1:200 dilution, P 0448, Dako) for 1 h at RT. Sections were mounted with Eukitt (Labonord, Villeneuve, D'ASCQ, France) after treatment with diamino-3,3′ benzidine. Digital images were captured using a CCD camera (Sony) and processed using Ellix software (Microvision, Evry, France).

Statistical analysis

Data for each group are represented as the mean plus standard deviation (s.d.). Differences between classes were determined using the Student's paired *t*-test. Differences between the percentages of increase in muscle mass or in SFA between WT and calpain 3-deficient mice were assessed using one-way ANOVA. All statistical tests were considered to be significant when the error was below 5%.

Acknowledgements

We thank the production and the *in vivo* departments of Généthon, especially Muriel Durand and Nicolas Guerchet. We also thank the Howard Hughes Medical Institute (Iowa City, IA, USA) for providing us with *Sgca*-null mice. We thank Elisabeth Baudoin for manuscript editing. This work was funded by the Association Française contre les Myopathies, the Centre National de la Recherche Scientifique, Genopole (Evry) and the Fondation pour la Recherche Médicale.

References

1 Grobet L, Martin LJ, Poncelet D, Pirottin D, Brouwers B, Riquet J *et al*. A deletion in the bovine myostatin gene causes the double-muscled phenotype in cattle. *Nat Genet* 1997; **17**: 71–74.

2 Kambadur R, Sharma M, Smith TP, Bass JJ. Mutations in myostatin (GDF8) in double-muscled Belgian Blue and Piedmontese cattle. *Genome Res* 1997; **7**: 910–916.

3 McPherron AC, Lee SJ. Double muscling in cattle due to mutations in the myostatin gene. *Proc Natl Acad Sci USA* 1997; **94**: 12457–12461.

4 Szabo G, Dallmann G, Muller G, Patthy L, Soller M, Varga L. A deletion in the myostatin gene causes the compact (Cmpt) hypermuscular mutation in mice. *Mamm Genome* 1998; **9**: 671–672.

5 Schuelke M, Wagner KR, Stolz LE, Hubner C, Riebel T, Komen W *et al*. Myostatin mutation associated with gross muscle hypertrophy in a child. *N Engl J Med* 2004; **350**: 2682–2688.

6 Clop A, Marcq F, Takeda H, Pirottin D, Tordoir X, Bibe B *et al*. A mutation creating a potential illegitimate microRNA target site in the myostatin gene affects muscularity in sheep. *Nat Genet* 2006; **38**: 813–818.

7 McPherron AC, Lawler AM, Lee SJ. Regulation of skeletal muscle mass in mice by a new TGF-beta superfamily member. *Nature* 1997; **387**: 83–90.

8 Zhu X, Hadhazy M, Wehling M, Tidball JG, McNally EM. Dominant negative myostatin produces hypertrophy without hyperplasia in muscle. *FEBS Lett* 2000; **474**: 71–75.

9 Yang J, Ratovitski T, Brady JP, Solomon MB, Wells KD, Wall RJ. Expression of myostatin pro domain results in muscular transgenic mice. *Mol Reprod Dev* 2001; **60**: 351–361.

10 Nishi M, Yasue A, Nishimatu S, Nohno T, Yamaoka T, Itakura M *et al*. A missense mutant myostatin causes hyperplasia without hypertrophy in the mouse muscle. *Biochem Biophys Res Commun* 2002; **293**: 247–251.

11 Grobet L, Pirottin D, Farnir F, Poncelet D, Royo LJ, Brouwers B *et al*. Modulating skeletal muscle mass by postnatal, muscle-specific inactivation of the myostatin gene. *Genesis* 2003; **35**: 227–238.

12 Whittemore LA, Song K, Li X, Aghajanian J, Davies M, Girgenrath S *et al*. Inhibition of myostatin in adult mice increases skeletal muscle mass and strength. *Biochem Biophys Res Commun* 2003; **300**: 965–971.

13 Walsh FS, Celeste AJ. Myostatin: a modulator of skeletal-muscle stem cells. *Biochem Soc Trans* 2005; **33**: 1513–1517.

14 Reisz-Porszasz S, Bhasin S, Artaza JN, Shen R, Sinha-Hikim I, Hogue A *et al*. Lower skeletal muscle mass in male transgenic mice with muscle-specific overexpression of myostatin. *Am J Physiol Endocrinol Metab* 2003; **285**: E876–E888.

15 Zimmers TA, Davies MV, Koniaris LG, Haynes P, Esquela AF, Tomkinson KN *et al*. Induction of cachexia in mice by systemically administered myostatin. *Science* 2002; **296**: 1486–1488.

16 Lee SJ. Regulation of muscle mass by myostatin. *Annu Rev Cell Dev Biol* 2004; **20**: 61–86.

17 Tobin JF, Celeste AJ. Myostatin, a negative regulator of muscle mass: implications for muscle degenerative diseases. *Curr Opin Pharmacol* 2005; **5**: 328–332.

18 Hill JJ, Davies MV, Pearson AA, Wang JH, Hewick RM, Wolfman NM *et al*. The myostatin propeptide and the follistatin-related gene are inhibitory binding proteins of myostatin in normal serum. *J Biol Chem* 2002; **277**: 40735–40741.

19 Wolfman NM, McPherron AC, Pappano WN, Davies MV, Song K, Tomkinson KN *et al*. Activation of latent myostatin by the BMP-1/tolloid family of metalloproteinases. *Proc Natl Acad Sci USA* 2003; **100**: 15842–15846.

20 Rebbapragada A, Benchabane H, Wrana JL, Celeste AJ, Attisano L. Myostatin signals through a transforming growth factor beta-like signaling pathway to block adipogenesis. *Mol Cell Biol* 2003; **23**: 7230–7242.

21 Zhu X, Topouzis S, Liang LF, Stotish RL. Myostatin signaling through Smad2, Smad3 and Smad4 is regulated by the inhibitory Smad7 by a negative feedback mechanism. *Cytokine* 2004; **26**: 262–272.

22 Patel K, Amthor H. The function of Myostatin and strategies of myostatin blockade-new hope for therapies aimed at promoting growth of skeletal muscle. *Neuromuscul Disord* 2005; **15**: 117–126.

23 Roth SM, Walsh S. Myostatin: a therapeutic target for skeletal muscle wasting. *Curr Opin Clin Nutr Metab Care* 2004; **7**: 259–263.

24 Khurana TS, Davies KE. Pharmacological strategies for muscular dystrophy. *Nat Rev Drug Discov* 2003; **2**: 379–390.

25 Engvall E, Wewer UM. The new frontier in muscular dystrophy research: booster genes. *FASEB J* 2003; **17**: 1579–1584.

26 Bogdanovich S, Krag TO, Barton ER, Morris LD, Whittemore LA, Ahima RS *et al*. Functional improvement of dystrophic muscle by myostatin blockade. *Nature* 2002; **420**: 418–421.

27 Wagner KR, McPherron AC, Winik N, Lee SJ. Loss of myostatin attenuates severity of muscular dystrophy in mdx mice. *Ann Neurol* 2002; **52**: 832–836.

28 Bogdanovich S, Perkins KJ, Krag TO, Whittemore LA, Khurana TS. Myostatin propeptide-mediated amelioration of dystrophic pathophysiology. *FASEB J* 2005; **19**: 543–549.

29 Holmes JH, Ashmore CR, Robinson DW. Effects of stress on cattle with hereditary muscular hypertrophy. *J Anim Sci* 1973; **36**: 684–694.

30 McMahon CD, Popovic L, Oldham JM, Jeanplong F, Smith HK, Kambadur R *et al*. Myostatin-deficient mice lose more skeletal muscle mass than wild-type controls during hindlimb suspension. *Am J Physiol Endocrinol Metab* 2003; **285**: E82–E87.

31 Li ZF, Shelton GD, Engvall E. Elimination of myostatin does not combat muscular dystrophy in dy mice but increases postnatal lethality. *Am J Pathol* 2005; **166**: 491–497.

32 Duguez S, Bartoli M, Richard I. Calpain 3: a key regulator of the sarcomere? *FEBS J* 2006; **273**: 3427–3436.

33 Roberds SL, Leturcq F, Allamand V, Piccolo F, Jeanpierre M, Anderson RD *et al*. Missense mutations in the adhalin gene linked to autosomal recessive muscular dystrophy. *Cell* 1994; **78**: 625–633.

34 Ozawa E, Mizuno Y, Hagiwara Y, Sasaoka T, Yoshida M. Molecular and cell biology of the sarcoglycan complex. *Muscle Nerve* 2005; **32**: 563–576.

35 Lim LE, Campbell KP. The sarcoglycan complex in limb-girdle muscular dystrophy. *Curr Opin Neurol* 1998; **11**: 443–452.

36 Kramerova I, Kudryashova E, Tidball JG, Spencer MJ. Null mutation of calpain 3 (p94) in mice causes abnormal sarcomere formation *in vivo* and *in vitro*. *Hum Mol Genet* 2004; **13**: 1373–1388.

37 Fougerousse F, Gonin P, Durand M, Richard I, Raymackers JM. Force impairment in calpain 3-deficient mice is not correlated with mechanical disruption. *Muscle Nerve* 2003; **27**: 616–623.

38 Bartoli M, Poupiot J, Goyenvalle A, Perez N, Garcia L, Danos O *et al*. Noninvasive monitoring of therapeutic gene transfer in animal models of muscular dystrophies. *Gene Therapy* 2006; **13**: 20–28.

39 Bartoli M, Roudaut C, Martin S, Fougerousse F, Suel L, Poupiot J *et al*. Safety and efficacy of AAV-mediated calpain 3 gene transfer in a mouse model of limb-girdle muscular dystrophy type 2A. *Mol Ther* 2006; **13**: 250–259.

40 Kramerova I, Kudryashova E, Venkatraman G, Spencer MJ. Calpain 3 participates in sarcomere remodeling by acting upstream of the ubiquitin-proteasome pathway. *Hum Mol Genet* 2005; **14**: 2125–2134.

41 Wang M, Orsini C, Casanova D, Millan JL, Mahfoudi A, Thuillier V. MUSEAP, a novel reporter gene for the study of long-term gene expression in immunocompetent mice. *Gene* 2001; **279**: 99–108.

42 Snyder RO, Miao CH, Patijn GA, Spratt SK, Danos O, Nagy D *et al*. Persistent and therapeutic concentrations of human factor

IX in mice after hepatic gene transfer of recombinant AAV vectors. *Nat Genet* 1997; **16**: 270–276.

43 Apparailly F, Khoury M, Vervoordeldonk MJ, Adriaansen J, Gicquel E, Perez N *et al*. Adeno-associated virus pseudotype 5 vector improves gene transfer in arthritic joints. *Hum Gene Ther* 2005; **16**: 426–434.

44 Zhang HG, Wang YM, Xie JF, Liang X, Hsu HC, Zhang X *et al*. Recombinant adenovirus expressing adeno-associated virus cap and rep proteins supports production of high-titer recombinant adeno-associated virus. *Gene Therapy* 2001; **8**: 704–712.

45 Fougerousse F, Bartoli M, Poupiot J, Arandel L, Durand M, Guerchet N *et al*. Phenotypic correction of α-sarcoglycan deficiency by intra-arterial injection of a muscle-specific serotype 1 rAAV vector. *Mol Ther* 2007; **15**: 53–61.

46 Duclos F, Straub V, Moore SA, Venzke DP, Hrstka RF, Crosbie RH *et al*. Progressive muscular dystrophy in alpha-sarcoglycan-deficient mice. *J Cell Biol* 1998; **142**: 1461–1471.

47 Richard I, Broux O, Allamand V, Fougerousse F, Chiannilkulchai N, Bourg N *et al*. Mutations in the proteolytic enzyme calpain 3 cause limb-girdle muscular dystrophy type 2A. *Cell* 1995; **81**: 27–40.

48 Gonin P, Arandel L, Van Wittenberghe L, Marais T, Perez N, Danos O. Femoral intra-arterial injection: a tool to deliver and assess recombinant AAV constructs in rodents whole hind limb. *J Gene Med* 2005; **7**: 782–791.